



Impact of Iron–Sulfur Clusters on the Spin–Lattice Relaxation Rate and ESEEM Frequency of the Oxidized Primary Donor P_{700}^{+} and Reduced Phylloquinone Acceptor A_1^{-} in Radical Pairs in Photosystem I Embedded in Trehalose Glassy Matrix

Andrey A. Sukhanov, et al. [full author details at the end of the article]

Received: 25 May 2020 / Revised: 16 June 2020 / Published online: 23 July 2020
© Springer-Verlag GmbH Austria, part of Springer Nature 2020

Abstract

ESEEM measurements were performed at two temperatures on Photosystem I (PS I) complexes depleted of the extrinsic PsaC subunit harboring iron–sulfur 4Fe–4S clusters F_A/F_B (abbreviated F_X -core complexes) embedded in trehalose glassy matrix. The ESEEM modulation frequencies obtained for the F_X -core complexes in trehalose matrix were similar at 150 K and 290 K. They correspond to a distance ~ 25 Å between the oxidized primary donor P_{700}^{+} and reduced phylloquinone acceptor A_1^{-} . This distance corresponds to the preferential charge separation pathway between P_{700}^{+} and A_{1B}^{-} in the *B*-branch of the PS I redox cofactors, while the distance estimated previously for the intact PS I complexes (containing the extrinsic PsaC subunit) embedded in dry trehalose matrix was ~ 26 Å, which is typical for the formation of $P_{700}^{+}A_{1A}^{-}$ charge-separated radical pairs in the symmetrical *A*-branch (Sukhanov et al. in Appl Magn Reson 49:1011, 2018). The redirection of electron transfer preferentially from the *A* to the *B*-branch of redox cofactors observed in F_X -core complexes embedded in dry trehalose matrix can be rationalized by the alteration of the protein domain rigidity/flexibility around phylloquinone molecules in the A_{1A} and A_{1B} sites, which affects the thermodynamics of electron transfer between P_{700} and A_1 in the symmetrical branches of cofactors. This finding of similar modulation frequencies measured for F_X -core complexes in trehalose matrix at 150 K and 290 K is opposite to our previously obtained results for intact PS I, where the value of ESEEM modulation frequency markedly decreased upon heating the sample from cryogenic to room temperature (Sukhanov et al. in Appl Magn Reson 49: 1011, 2018). Our comparison of F_X -core complexes with intact PS I complexes suggests that 4Fe–4S clusters accelerate spin–lattice relaxation of the unpaired electron spins on the phylloquinone in the A_1 -site. The result serves as additional argument in favor of the molecular model of the cryoprotective effect of trehalose matrix on the functioning of PS I by way of rigidity changes of the hydrogen-bonding network of the protein with the matrix that is based on the Le Chatelier–Braun principle. According to this thermodynamic principle, changes in both rigidity and flexibility are compensated to establish new thermodynamic equilibria

with restored global balance of rigidity and flexibility that is typical within functioning protein complexes.

1 Introduction

The pigment–protein complex of Photosystem I (PS I) acts as plastocyanin/ferredoxin/flavodoxin oxidoreductase in thylakoid membranes of cyanobacteria and chloroplasts. In 2001, Jordan and coworkers [2] provided the first complete X-ray structure of trimeric PS I from the thermophilic cyanobacterium *Thermosynechococcus elongatus*, providing a full glimpse of the reaction center (RC) cofactors. They displayed the positions of 12 protein subunits for each monomer and their interactions with redox cofactors. The membrane-spanning core consists of two large protein subunits (PsaA and PsaB) that bind 85 chlorophyll (Chl) *a* molecules (from the total 96), 22 β -carotene molecules, two phylloquinone molecules, and the 4Fe–4S cluster F_X . The majority of Chl *a* molecules function as a light-harvesting antenna. The terminal 4Fe–4S clusters F_A and F_B are bound to the peripheral small subunit PsaC.

The reducing potential required for generating a strong reductant, NADPH is derived from the light-induced electron transfer along a series of cofactors bound to the PsaA and PsaB subunits of PS I. In so doing, the primary process of charge separation culminates with a hole at the primary donor P_{700} (a Chl *a*/Chl *a'* heterodimer) and an electron at the primary acceptors A_{0A}/A_{0B} in the symmetrical branches of cofactors *A* and *B* (which are represented by two pairs of Chl *a* molecules). This initial charge-separated state is stabilized by electron transfer to the secondary acceptors A_{1A}/A_{1B} (phylloquinone molecules), then to 4Fe–4S F_X cluster ligated between the PsaA/PsaB heterodimer, and further to the terminal acceptors, the 4Fe–4S clusters F_A/F_B .

The study of the influence of the disaccharide bioprotectors on the photosynthetic RC complexes is of particular interest [3–6]. Trehalose, a nonreducing disaccharide, which is naturally produced by several species of eubacteria, archaea, some fungi, certain invertebrates, green algae, and plants, has attracted increased attention due to its unique physical–chemical properties enabling long periods of life without water (*anhydrobiosis*). Trehalose as glassy matrix inhibits protein denaturation caused by freezing, heating, and drying [3–6]. The existing paradigm of the protective mechanism of the native protein structure by trehalose is based on the assumption that trehalose inhibits protein dynamics already at room temperature [7, 8]. This assumption was proved by comparison of the electron transfer kinetics in PS I complexes in glycerol–water solution upon temperature decrease and upon relative humidity decrease in trehalose glassy matrix [5, 9, 10]. A number of similarities were apparent in the charge recombination kinetics of PS I immobilized in glycerol glass at 170 K and trehalose glass at 298 K. The slowing down of electron transfer in the trehalose and glycerol mixtures could probably be caused by similar physical processes that take place within and around the protein globule, namely, a glass transition of the surrounding medium. Note that trehalose is distinguished from other sugars by an extremely high glass-transition temperature of ~ 380 K. However, the

molecular mechanism of the trehalose glassy matrix influence on the protein functioning remains a matter of debate.

Despite the large attention devoted to the anhydrobiosis and biopreservation phenomena, the molecular mechanisms are still unclear, in particular the molecular basis of the extraordinary efficiency of trehalose matrix. Extensive experimental work, employing for instance neutron scattering, Raman optical laser-flash, FTIR, and EPR spectroscopy on different proteins incorporated into trehalose glasses, has revealed a tight protein–matrix dynamic coupling at low water content, implying that the protein conformational dynamics is controlled by that of the water–trehalose matrix. Proteins embedded in water–saccharide amorphous matrices have provided evidence of a tighter protein–matrix coupling to trehalose than to sucrose and other sugars (for references, see for example [6, 8]). This large body of studies has led to several (not mutually exclusive) hypotheses, in which different factors have been considered as predominant in determining the bioprotective effects: (1) stabilization via direct hydrogen-bonding between the sugar and the biostructure (water-replacement hypothesis); (2) entrapping of residual water molecules at the biomolecule–disaccharide interface (water-entrapment hypothesis); (3) increased rigidity via the extraordinary viscosity increase upon vitrification (vitrification hypothesis); (4) tight anchorage of the protein surface to the stiff matrix by residual water molecules, constrained at the protein–matrix interface by a network of H-bonds simultaneously connecting surface protein groups and disaccharide molecules (anchorage hypothesis). According to the widely favored anchorage model, the intimate interactions of different disaccharides with water and with the biomolecule via H-bonding are expected to modulate the protein–matrix dynamical coupling essential for forming functional pathways for protein functioning and, consequently, controlling the effectiveness of bioprotection.

In an attempt to clarify the role of protein–water–sugar interaction for biological function of PS I complexes under external changes, we considered phenomenologically the possibility that under adverse stress conditions trehalose prevents significant changes of the static structure of the PS I protein but allows for functionally important changes of the conformational dynamics of PS I due to changes of the rigidity \leftrightarrow flexibility equilibrium of the protein–matrix complex, thereby providing reversibility of the stress-induced changes.

In order to check whether this is a viable possibility, we used time-resolved pulsed EPR spectroscopy to accurately measure the distance between unpaired electrons of paramagnetic radical-pairs in the range of 1.5–8 nm as well as the spin–lattice relaxation time of unpaired electrons on a radical center. In our case, we specifically compared the $P_{700}^+A_1^-$ radical-pair and the A_1^- radical anion in intact PS I RCs with those in F_X -core complexes, both embedded in trehalose glassy matrix. F_X -core complexes are modified PS I complexes depleted of the extrinsic PsaC subunit harboring terminal iron-sulfur 4Fe–4S clusters F_A/F_B . By removing the iron-sulfur 4Fe–4S clusters F_A/F_B , the spin–lattice relaxation rate of the A_1^- radical anion is expected to be strongly reduced.

The use of EPR spectroscopy for determining the structural characteristics of RCs, for example, the distance between separated spins in charge-separated radical-pairs, is based on measuring the energy of the spin–spin dipole–dipole interaction

between the separated spins. The energy of the dipole–dipole spin interaction determines the frequency of the electron spin envelope echo modulation decay of the primary electron spin echo signal (ESEEM effect) of the separated charges in the RC [1].

Using the ESEEM method, it was shown [1] that the ESEEM modulation frequency decreases with increasing temperature from 150 K to room temperature in the intact PS I complexes embedded into trehalose glassy matrices. However, it was previously demonstrated [5] that the W-band EPR spectra of the spin-correlated radical pair $P_{700}^+ A_1^-$, as measured in a dehydrated trehalose-PS I matrix at 293 K and 120 K, and in an aqueous buffer solution of PS I frozen at 120 K in the presence of glycerol, are essentially identical, revealing that the structural configuration of the transient radical pair does not change significantly upon solvation in the different matrices embedding the PS I complex.

Therefore, in order to explain the observed decrease in signal modulation frequency, we suggested that due to random spin flips during spin–lattice relaxation in the experiment, the modulation frequency of the spin echo signal is lower than the dipole frequency itself, as it was theoretically shown by [11, 12]. This effect is similar to the well-known decrease of the frequency of oscillation of a pendulum due to friction. In the PS I RC, the spins of the separated charges must have different spin–lattice relaxation rates, since the electron spin on the quinone interacts with the spins of the iron–sulfur clusters. Therefore, it can be expected that the 4Fe–4S clusters located at the acceptor side of PS I make a significant contribution to the spin–lattice relaxation of an electron on quinone, so that with increasing temperature the spin–lattice relaxation time of the quinone anion radical will decrease. Magnetic iron complexes can create rapidly fluctuating local dipolar magnetic fields at the location of the electron spin on the acceptor A_1^- and thus accelerate paramagnetic relaxation of the A_1^- electron spin.

In this case, according to the theory [11, 12], with increasing temperature, the modulation frequency of the spin echo signal should decrease even if the distance between the spins does not change. Theoretical calculations of the modulation frequency of the spin echo signal and the comparison with the frequencies measured in the experiment showed that to explain the observed frequency shift when heated from 150 K to room temperature, it is sufficient to assume that the relaxation time of the electron spin on the quinone decreases by a factor of 3 (from 3 to 1 μ s).

Such values of the spin–lattice relaxation time of the electron spin of reduced quinone are typical for organic radicals and radical ions. Therefore, in [1], it was concluded that the decrease in the modulation frequency of the electron spin echo signal observed in the PS I complexes when heated from 150 K to room temperature can be attributed to a decrease in the frequency (red shift of the modulation frequency) due to the acceleration of the spin–lattice relaxation of the electron spin, rather than to an increase in the distance between the spins due to thermal expansion of the complex.

Based on our experimental results and the data available in the literature, we proposed a phenomenological molecular model of the stabilizing and cryoprotective effect of trehalose on the functioning of PS I [1]. This model assumes the existence of two variants of adsorption of trehalose on the protein surface, endothermic

and exothermic, which may differ either because of a different conformation of the trehalose–protein complex or because of a different realization of hydrogen bond networks of the protein with surrounding trehalose molecules. Then, the discussed effect of trehalose on the functioning of the RC can be explained by the Le Chatelier–Braun principle. Accordingly, the rigidity ↔ flexibility equilibria of protein–matrix complexes adjust via this principle to restore the global balance of rigidity and flexibility necessary for functioning of protein structures. This is achieved by establishing enthalpy–entropy compensation, where weakening the H-bond network in the native-state ensemble (enthalpy effect) is compensated by a corresponding increase in flexibility (entropy effect) [13]. Our results indicate that balancing rigidity and flexibility along the backbone is essential for preserving biological function of the PS I protein–matrix complex.

To justify the model, the influence of 4Fe–4S clusters on the spin–lattice relaxation of separated charges in PS I RCs is of fundamental importance. In this work, we estimated the spin–lattice relaxation lifetimes of separated charges in PS I complexes depleted of extrinsic protein subunit PsaC carrying the terminal 4Fe–4S clusters F_A/F_B , and embedded in trehalose glassy matrices at different temperatures.

2 Materials and Methods

Wild-type strain of *Synechocystis* sp. PCC 6803 cells were grown as described previously [14]. Cells were broken using a French pressure cell operated at 4 °C at 120 MPa. Thylakoid membranes were solubilized using n-dodecyl-β-D-maltopyranoside (β-DM), and PS I trimers were isolated by sucrose density ultracentrifugation according to previously published procedures [14]. Samples were finally resuspended in 50 mM Tris–HCl (pH 8.0) buffer containing 0.03% (w/v) β-DM and 15% (v/v) glycerol at Chl concentration 1.5–2.0 mg mL⁻¹, and stored at –80 °C until required.

Trehalose-PS I glassy matrices were prepared following essentially the procedures for the incorporation of bacterial RCs into trehalose glassy matrix [6]. In doing so, the trehalose/PS I molar ratio was 40.000 and the relative humidity of 11% was achieved in ~14 days (see [5] for details).

The $A_1^{\cdot-}$ spin–lattice relaxation time of the reduced phylloquinone acceptors $A_1^{\cdot-}$ and the distance between the separated charges and electron spins in the laser-pulse generated radical-pairs $P_{700}^{\cdot+} A_1^{\cdot-}$ of the oxidized primary donor $P_{700}^{\cdot+}$ and the reduced phylloquinone acceptor $A_1^{\cdot-}$ in the intact PS I and F_X -core complexes were measured by the pulsed EPR method of the stimulated electron spin echo (ESEEM). The measurements were carried out at Q-band frequency (33.72 GHz) [1]. We used the Bruker Elexsys E580 EPR spectrometer equipped with the resonator ER 5106QT-E and the Bruker Temperature Control System ER 4131VT. Intra-cavity photoexcitation of the RC complexes was performed with a Quantel Brio Nd:YAG laser. The pulse energy at 532 nm output wavelength exceeds 45 mJ with pulse duration of 7 ns and 20 Hz repetition rate; for the current experiments the pulse energy was reduced to 2 mJ/pulse on the sample surface.

3 Theoretical Basis for Determining Interspin Distances in Radical-Pairs by ESEEM

To measure the distance in the radical-pair $P_{700}^{+} A_1^{-}$ of PS I, the modulation effect of the primary spin echo envelope decay was used. Measurements were performed at various temperatures. In the experiment, a nonmonotonic decrease in the echo signals appears with increasing time interval τ between the microwave pulses forming the echo signal, manifesting the ESEEM effect. This modulation effect is caused by a spin–spin dipole–dipole interaction between the separated $P_{700}^{+} A_1^{-}$ charges in PS I RC. The dipole–dipole interaction depends on the distance r between the separated charges as $1/r^3$ (see spin Hamiltonian (1)):

$$H_{d-d} = ((g_1 g_2 \beta^2 (1 - 3 \cos^2 \theta) / r^3) / \hbar) S_{1z} S_{2z} \quad (1)$$

where g_k , S_{kz} , $k=1,2$, denote isotropic g -factors and projections of the operator of the electron spin moment of the separated charges on the direction of the external constant magnetic field B_0 , which is chosen as the axis of quantization of spins, β is the Bohr magneton, θ is the angle between the direction of the external magnetic field and a radius vector connecting the electron spins on the PS I photooxidized primary electron donor, a chlorophyll *a* special pair (P_{700}^{+}), and reduced phylloquinone electron acceptor (A_1^{-}).

It is well known that the decay of the signal of the primary electron spin echo of the separated charges oscillates with a frequency determined by the spin–spin dipole–dipole interaction between the separated charges in the RC on the condition that the microwave pulses forming the echo signal excite the spins of both separated charges [12]. Then, the expected ESEEM frequency of the primary spin echo signal is given by

$$\omega_{d-d} = (g_1 g_2 \beta^2 (1 - 3 \cos^2 \theta) / r^3) / \hbar \quad (2)$$

Thus, the ESEEM frequency depends on the distance r between the spins of the separated charges and on the orientation of the RC relative to the direction of the external magnetic field. In our experiments, the RCs in the sample are randomly oriented. Therefore, there is a spread in the ESEEM frequencies for RCs oriented differently in space. But the modulation frequency distribution function has a peculiarity: the frequency that corresponds to the orientation $\theta = \pi/2$ and to θ in the vicinity of $\pi/2$ [15] has the largest statistical weight in the ESEEM effect, and this frequency equals

$$\omega_{d-d} = \Omega = (g_1 g_2 \beta^2 / r^3) / \hbar \quad (3)$$

From experiments on the electron spin echo, one can find the ESEEM frequency and then use the formula (3) to determine the distance between two separated charges, i.e., in the case studied between the spins on the primary cofactors P_{700}^{+} and A_1^{-} of the RC.

However, in the experiment, the observed modulation frequency of the decay of the echo signals may slightly differ from the dipole–dipole frequency (3). It

was theoretically shown [11, 12] that, due to random spin flips during spin–lattice relaxation in the experiment, the modulation frequency of the spin echo signal is lower than the dipole frequency itself. This effect is similar to the well-known reduction of the frequency of oscillations of a pendulum under friction.

In the RC, it is expected that the spins of the separated charges must have different spin–lattice relaxation rates, since the electron spin on the quinone interacts with the spins on the iron–sulfur clusters. According to the theory of Salikhov and coworkers [12], in the decay of the ESEEM signal in PS I, the dipole–dipole interaction between the spin on P_{700}^{+} and the spin on A_1^{-} contributes to:

$$V_{dd}(2\tau) = \left[\left(\cos(R\tau) + \frac{1}{2T_1R} \sin(R\tau) \right)^2 + \left(\frac{\omega_{d-d}}{2R} \right)^2 \sin^2(R\tau) \right] \exp(-\tau/T_1) \quad (4)$$

In Eq. (4), T_1 is the spin–lattice relaxation time of the electron spin on A_1^{-} , φ is the angle of spin rotation on A_1^{-} induced by the second microwave pulse, which forms the primary spin echo of the electron spin on P_{700}^{+} , R is given as

$$R = (1/2)\omega_{d-d} \sqrt{1 - 1/(\omega_{d-d}T_1)^2} \quad (5)$$

In the case of separated charges in the RC, the lines of the EPR spectra of P_{700}^{+} and A_1^{-} only slightly overlap; therefore, in experiments on the observation of the spin echo signal of spins on P_{700}^{+} , the probability $p \leq \sin^2(\varphi/2) >$ of the A_1^{-} microwave spin excitation by pulses forming the observed echo signal should be significantly less than one.

It is seen from Eq. (4) that for the manifestation of the dipole–dipole interaction between the spins of the separated charges in the form of a modulation of the decay of the spin echo envelope, both the excitation pattern of the spins of a pair by the microwave pulses forming the echo signal and random spin flips caused by the spin–lattice relaxation, are important.

Assume that the spin–lattice relaxation rate is zero. Then Eq. (4) turns to

$$V_{dd}(2\tau) = (1 - p + p \cos(\omega_{d-d}\tau)) \quad (6)$$

This equation is well known in the theory of pulsed double electron–electron resonance (PELDOR, see, for example, [15]). It is seen from Eq. (6) that without random spin flips during spin–lattice relaxation, a dipole–dipole interaction induces modulation of the spin echo signal only if microwave pulses excite both spins of the interacting pair, $p > 0$.

If the microwave pulses forming the spin echo signal of one radical-pair partner do not excite the spin of the other radical-pair partner, i.e., when in Eq. (4) $p \leq \sin^2(\varphi/2) \geq 0$, then the contribution of the dipole–dipole interaction in a pair of separated charges to the decay of the spin echo signal is described by [11, 12]:

$$V_{dd}(2\tau) = \left[\left(\cos(R\tau) + \frac{1}{2T_1R} \sin(R\tau) \right)^2 + \left(\frac{\omega_{d-d}}{2R} \right)^2 \sin^2(R\tau) \right] \exp(-\tau/T_1) \tag{7}$$

In contrast to the situation in Eq. (6), according to Eq. (7) random spin flips during spin–lattice relaxation can cause modulation of the decay of spin echo signals even if $p=0$ for sufficiently long spin–lattice relaxation times T_1 , i.e., under conditions when

$$\omega_{d-d}T_1 > 1 \tag{8}$$

According to Eqs. ((4), (8), the modulation of the decay of the electron spin echo signals is described by the terms containing $\sin(2R\tau)$ and $\cos(2R\tau)$, which oscillate with a frequency of

$$\Omega_{\text{mod}} = 2R = \omega_{d-d} \sqrt{1 - 1/(\omega_{d-d}T_1)^2} \tag{9}$$

Thus, under the condition $\omega_{d-d} T_1 \gg 1$, the ESEEM frequency approaches the dipole–dipole frequency ω_{d-d} .

It is worth noting that under the condition $\omega_{d-d} T_1 \leq 1$, the ESEEM effect disappears.

We see that the ESEEM frequency of the spin echo signal is equal to the dipole frequency only when the spin–lattice relaxation time is long enough. Otherwise, the observed ESEEM frequency has a red frequency shift. Hence, one should take into account that, in order to determine the dipole frequency from the data on the modulation of the spin echo signal decay, it is necessary to determine the spin–lattice relaxation time of the spins from independent experiments as follows:

(1) To determine the spin–lattice relaxation time, various EPR spectroscopy techniques can be used. A widely used method is observing the recovery of equilibrium longitudinal magnetization of spins after magnetization inversion induced by a short microwave pulse. In this case, the magnetization is recovering according to the law (see Fig. 3)

$$M_z(T) = -M(0) \exp(-T/T_1) + M_0(1 - \exp(-T/T_1)) \tag{10}$$

In this equation, $M(0)$ is the initial magnetization of the system created by a short microwave pulse, M_0 is the equilibrium magnetization. Note that cross relaxation processes can lead to a more complex kinetics of magnetization recovery.

(2) Another established method for measuring spin–lattice relaxation time is the stimulated spin echo method. According to [11, 12] the dipole–dipole spin–spin interaction contributes to the stimulated echo signal of A_1^- as given by Eq. (11):

$$V_{dd}(2\tau, T) = V_0 \left[\left(\cos(R\tau) + \frac{1}{2T_{1p}R} \sin(R\tau) \right)^2 + \exp\left(-\frac{T}{T_{1p}}\right) \left(\frac{\omega_{d-d}}{2R} \right)^2 \sin^2(R\tau) < \cos(\varphi_2) \cos(\varphi_3) > \right] \exp(-\tau/T_{1p}) \tag{11}$$

Here φ_2 and φ_3 are the angles of spin rotation on P_{700}^+ induced by the second and third microwave pulses (see Eq. 4).

The stimulated echo signal contains a term proportional to $\exp(-T/T_1)$. By studying the time T dependence of the stimulated spin echo signal one can determine the spin–lattice relaxation time T_1 of the A_1^- spins.

But Eq. (11) presents only contribution of the dipole–dipole interaction between spins in the $P^+A_1^-$ pair to the A_1^- spin echo signal decay. The main dependence on spin–lattice relaxation time T_1 of the A_1^- stimulated spin echo signal arises from the spin–lattice relaxation of A_1^- spins themselves. Indeed, there is decay of the A_1^- stimulated echo signal induced by the inherent transverse, T_{2A_1} , and longitudinal, T_{1A_1} , relaxation processes of A_1^- spins. Taking into account spin–lattice relaxation of A_1^- spins, the stimulated echo decay is given as

$$V(2\tau, T) = V_{\text{dd}}(2\tau, T)\exp(-2\tau/T_{2A_1})\exp(-T/T_{1A_1}) \quad (12)$$

So, the stimulated echo signal contains a term proportional to $\exp(-T/T_{1A_1})$. By studying the time T dependence of the stimulated spin echo signal one can determine the spin–lattice relaxation time T_1 of the A_1^- spins.

4 Experimental Data and Their Discussion

4.1 Estimation of the Spin–Lattice Relaxation Time of Reduced Phylloquinone

A_1^-

To measure the distance between the separated charges in the $P_{700}^+ A_1^-$ radical pair, we use the ESEEM frequency of the P_{700}^+ . This frequency is determined by two quantities: the frequency of the spin–spin dipole–dipole interaction on the one hand, and the spin–lattice relaxation rate of the unpaired electron on the reduced A_1^- phylloquinone on the other hand (see Eq. 9). Generally speaking, the modulation frequency also depends on the spin–lattice relaxation rate of the electron hole on the oxidized P_{700}^+ Chl dimer, but this is quite small, and the contribution of the P_{700}^+ spin–lattice relaxation to the red shift of the echo signal modulation frequency can be neglected.

To measure the A_1^- spin–lattice relaxation time in our experiments, we used the pulse EPR method of the stimulated electron spin echo signal. The experimental protocol is shown in Fig. 1. The measurements were carried out at Q-band microwave frequency (33.72 GHz) [1].

Two types of experiments were performed. In the first experiment, which allows one to measure the spin–lattice relaxation time, the delay T between the last two microwave pulses was changed in the pulse protocol with a constant delay after the laser flash (DAF). In this experiment, the minimum delay of 500 ns after the laser pulse was used, which depends only on the operation rate of the EPR spectrometer trigger. In the second experiment, the delay T was constant and amounted to 300 ns, while the delay after laser pulse varied; the duration of the $\pi/2$ microwave pulse was 28 ns.

The measurements were performed at a magnetic field corresponding to the resonance position of the A_1^- radical (indicated by an asterisk in Fig. 2) at

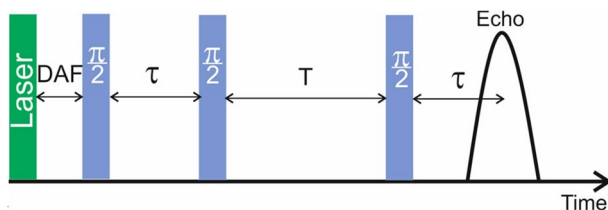


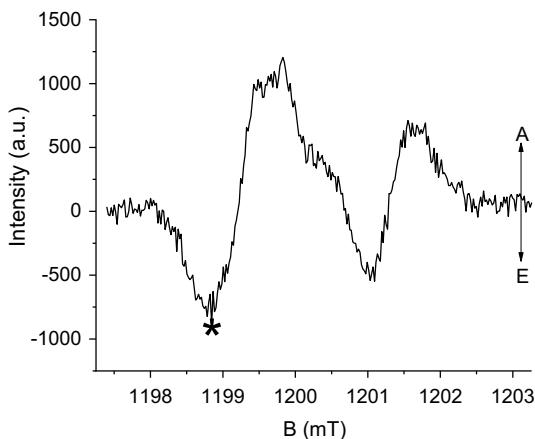
Fig. 1 Schematic pulse protocol of the experiment for measuring the spin–lattice relaxation time of laser-flash generated reduced phyloquinone $A_1^{\cdot-}$ in the intact PS I RC and F_A/F_B -depleted PS I (F_X -core complexes) embedded in dry trehalose matrix. The laser pulse at time $t=0$ creates radical pairs of separated charges. After some delay (*DAF*, delay after flash), a sequence of three microwave pulses is applied, which form the signal of the stimulated electron spin echo. The variable times τ and T are the delays between the first and second and between the second and third microwave pulses, respectively. The $\pi/2$ microwave pulses excite predominantly the electron spins of $A_1^{\cdot-}$

temperatures 150 K and 290 K. Note that, as a result of the recombination of the $P_{700}^+ A_1^{\cdot-}$ pair, the intensity of the observed signal with increasing T interval should also decrease due to a decrease in the number of pairs of separated charges. Therefore, not only the spin–lattice relaxation, but also the decay of the radical pairs due to their recombination contributes to the decay of the stimulated spin echo signal with increasing T (see Eq. (12)). Hence, the observed decay of the spin-echo signal gives the lowest estimate of the spin–lattice relaxation time value.

Figure 3 shows the time dependence of the intensity of the stimulated echo signal of $A_1^{\cdot-}$ in F_X -core complexes at 150 K and 290 K.

At 150 K, the spin–lattice relaxation time T_1 is larger than 6 μ s. Estimates using Eq. (8) show that, at $T_1 > 6 \mu$ s, spin–lattice relaxation gives only a negligible contribution to the modulation frequency of the spin echo signal for separated charges in the RC. As expected, upon temperature increase, the decay time of the echo signal decreases and, as deduced from Fig. 3, it becomes equal to $\sim 2 \mu$ s.

Fig. 2 The time-resolved spin-polarized EPR spectrum of PS I F_X -core complexes at room temperature in a time window of 0.3–1.2 μ s after the laser pulse. The measurements were performed at a magnetic field corresponding to the resonance position of the laser light-generated $A_1^{\cdot-}$ radical (indicated by an asterisk). In the spin-polarized EPR spectrum, A stands for absorption, E for emission



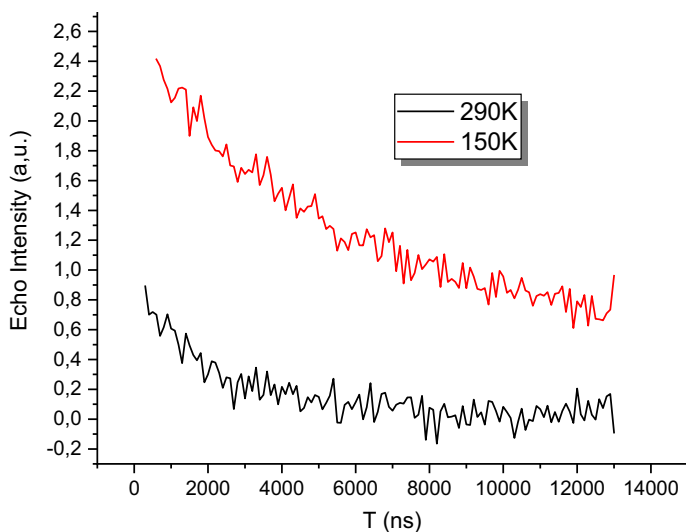


Fig. 3 The dependence of the intensity of the stimulated echo of $A_1^{\cdot-}$ as a function of time T for the F_X -core complexes in dried trehalose matrix at 150 K (red trace) and 290 K (black trace)

Thus, for PS I depleted of F_A/F_B iron–sulfur centers, we obtain an estimate for the spin–lattice relaxation time of $T_1 > 2 \mu\text{s}$. Such a relatively slow spin–lattice relaxation cannot cause a noticeable red shift in the modulation frequency. Therefore, in experiments with PS I lacking 4Fe–4S complexes, we do not observe a shift in the modulation frequency of the spin echo signal. As we have previously shown [1], in intact PS I complexes containing terminal F_A/F_B clusters dried in trehalose matrix, at a low temperature (150 K), the decay time of the echo signal was $T_1 > 5 \mu\text{s}$. But at 290 K, the echo signal was not observed because its lifetime was less than 0.6 μs , which is the time interval necessary for the formation of the stimulated spin echo and corresponds to the duration of the sequence of the three microwave pulses [1].

4.2 Distance Between the Separated Charges and Spins in the Radical Pair $P_{700}^{\cdot+} A_1^{\cdot-}$ in F_A/F_B -Depleted PS I Complexes in Dry Trehalose Matrix

In intact PS I complexes containing the terminal iron-sulfur clusters F_A/F_B , we observed a decrease in the frequency of modulation of the decay of the $P_{700}^{\cdot+}$ spin echo signal upon temperature increase from 120 K to room temperature [1]. Taking into account the above results of the theory of manifestation of the dipole–dipole interaction in a spin-echo signal, we concluded that the decrease in frequency of the ESEEM signal with temperature increase in the glassy trehalose matrix does not necessarily imply an increase in the distance between $P_{700}^{\cdot+}$ and $A_1^{\cdot-}$ spins. As we suggested earlier, this observation can be attributed to the influence of spin–lattice relaxation of $A_1^{\cdot-}$ [1]. Our calculations showed that the observed effect requires a decrease in the spin–lattice relaxation time from 3 to 1 μs when heated from 150

to 290 K. We proposed that the spin–lattice relaxation time of $A_1^{\cdot-}$ may depend on the charged paramagnetic $4Fe-4S$ clusters F_A/F_B located within 20–25 Å from A_1 . In order to check this hypothesis, we studied the temperature dependence of the ESEEM frequency of the primary spin echo signal in F_A/F_B -depleted PS I complexes (F_X -core complexes) in dried trehalose matrices. Figure 4 shows the experimental data.

The modulation frequencies for the experiments performed at 150 K and 290 K were estimated from the Fourier transform of the decay curves shown in Fig. 4, as presented in Fig. 5.

From the magnitude of the modulation frequency, the distance between the separated charges of radical pairs $P_{700}^{\cdot+} A_1^{\cdot-}$ in F_X -core complexes was calculated according to Eq. (9). The results are presented in Table 1.

The data presented in Fig. 4 and Table 1 show that the frequency of the ESEEM signal does not change in F_A/F_B -depleted PS I complexes dried in trehalose matrix, when the temperature changes from 150 to 290 K. Accordingly, the distance between the separated charges does not change under sample heating in this temperature range. This result contradicts the data obtained with the intact (F_A/F_B -containing) PS I complexes at 290 K, where the modulation frequency and accordingly the estimated distance between $P_{700}^{\cdot+}$ and $A_1^{\cdot-}$ increased by ~ 1 Å compared to the distance at 150 K [1]. However, as was suggested by Sukhanov et al. [1], this effect can be attributed to the influence of decreased spin–lattice relaxation time T_1 of $A_1^{\cdot-}$ from ~ 3 μs to 0.8 μs . The data presented in Fig. 3 show that the relaxation time T_1 in F_X -core samples used in this work at 290 K is ~ 2 μs . As mentioned above, this relatively slow spin–lattice relaxation cannot cause a noticeable red shift in the ESEEM

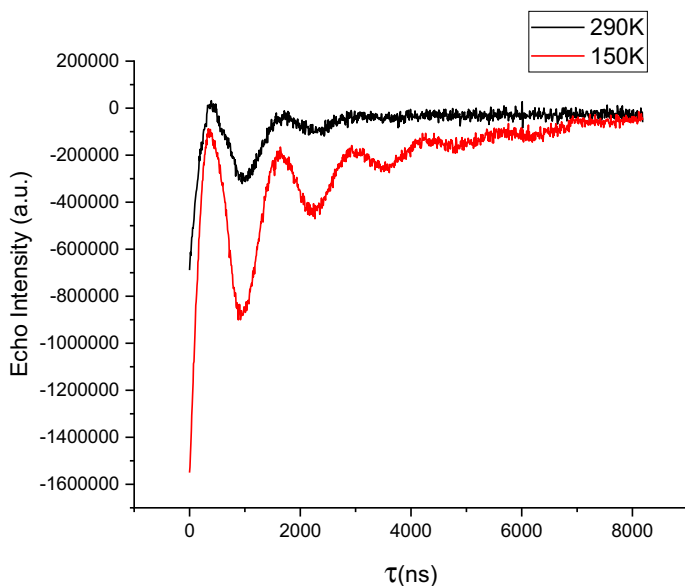


Fig. 4 Modulation of the primary spin-echo signal decays of radical pairs $P_{700}^{\cdot+} A_1^{\cdot-}$ for PS I F_X -core complexes in dried trehalose matrix at 150 K and 290 K

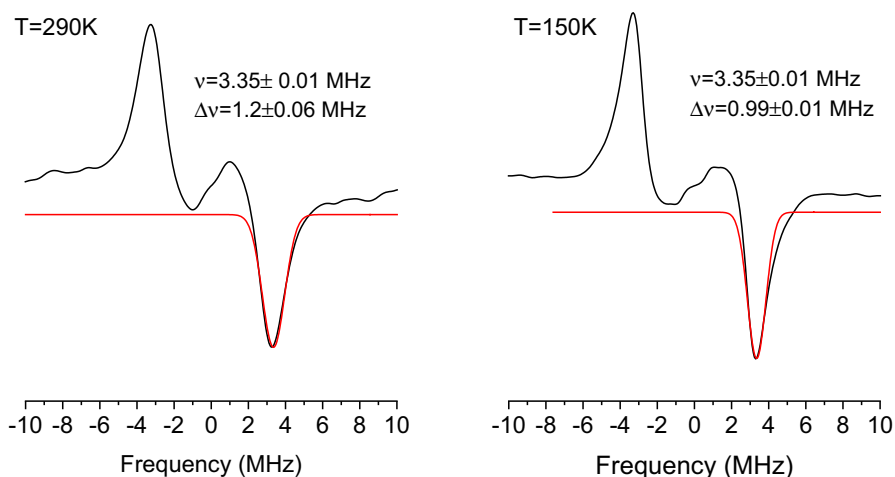


Fig. 5 Fourier transform of the modulated electron spin-echo signal decays shown in Fig. 4

Table 1 Temperature dependence of the ESEEM frequency of spin-correlated radical pairs $P_{700}^+ A_1^-$ and distance between separated charges in F_X -core PS I complexes in dried trehalose matrix

Temperature (K)	ESEEM frequency (MHz)	Distance R_{P-A} (Å)
290	3.35 ± 0.01	24.95 ± 0.07
150	3.35 ± 0.01	24.95 ± 0.07

modulation frequency and consequently does not affect the estimation of the distance between P_{700}^+ and A_1^- .

It is noticeable that the distance between P_{700}^+ and A_1^- , $R(P_{700}^+ A_1^-)$, estimated for samples in water-glycerol solution and in dry trehalose matrix for the intact (F_A/F_B -containing) PS I complexes at cryogenic temperatures was ~ 26 Å [1, 16], while for F_X -core samples embedded into glassy trehalose (this work) this distance was estimated as ~ 25 Å, both at room and at cryogenic temperature. This discrepancy requires some explanation.

As was previously shown, the spin-density distribution in the “special pair” cation-radical P_{700}^+ is shifted noticeably towards the *B*-side Chl molecule of the P_{700} dimer [17, 18], and assuming that the center of gravity of the spin-density distribution in the anion-radicals A_{1A}^- and A_{1B}^- is located in the center of quinone rings, the X-ray structure data of PS I suggest the following center-to-center distances: $R(P_{700}^+ A_{1A}^-) = 25.8$ Å and $R(P_{700}^+ A_{1B}^-) = 24.6$ Å [2]. Thus, the $R(P_{700}^+ A_1^-)$ value obtained for the intact PS I in trehalose matrix (~ 26 Å) roughly corresponds to $R(P_{700}^+ A_{1A}^-)$, while the distance value for F_X -core complexes in trehalose matrix (~ 25 Å) corresponds to $R(P_{700}^+ A_{1B}^-)$. There are two possible explanations of this difference:

For one thing, the asymmetric electron transfer along the *A* branch of redox cofactors in PS I at room temperature ($\sim 3:1$ in favor of the *A*-branch compared to

the *B*-branch) becomes almost symmetric ($\sim 1:1$) in F_X -core complexes [10]. This is most probably due to the lack of the extrinsic PsaC subunit in F_X -core samples, which carries asymmetrically distributed charged amino acid residues affecting the redox-potentials E_m of A_{1A} and A_{1B} . The other factor responsible for the difference in E_m values of the phyloquinone molecules in the A_{1A} and A_{1B} sites is the asymmetrical arrangement of the negatively charged F_A and F_B clusters towards A_{1A} and A_{1B} [19]. According to the data obtained by flash spectrometry at 830 nm, the relative contribution of recombination of $P_{700}^+A_{1B}^-$ ion-radical pairs in dry trehalose matrix increases at the expense of recombination from A_{1A}^- to P_{700}^+ , and this increase in F_X -core complexes is 2.5 times more pronounced compared to the intact PS I complexes in favor of the *B*-branch [9]. As was suggested from the observed X-ray structure in Ref.[9], the local pool of the intraprotein bound water molecules in the vicinity of the A_{1A} -site is more accessible to the external water phase than in the vicinity of A_{1B} , especially in the F_X -core complexes. Therefore, it is safe to suggest that the observed decrease of the distance between P_{700}^+ and A_1^- from ~ 26 Å in intact PS I to ~ 25 Å in F_X -core complexes embedded in trehalose glass at 11% humidity is due to the change of the predominant electron transfer pathway from the *A* to the *B* branch of redox cofactors in PS I.

5 Conclusions

The comparison of the dynamics of spin–lattice relaxation obtained with intact and F_X -core PS I complexes in dry trehalose matrices show that the increase of spin–lattice relaxation rate upon heating from cryogenic to room temperature in F_X -core complexes is less pronounced and, therefore, cannot cause a noticeable red shift in the ESEEM modulation frequency. Hence, in contrast to the intact PS I complexes, in F_X -core PS I complexes this increase does not affect the estimation of the distance between P_{700}^+ and A_1^- based on ESEEM methods. The modulation frequencies estimated for F_X -core complexes in trehalose matrix were similar at 150 K and 290 K and corresponded to a distance between P_{700}^+ and A_1^- of ~ 25 Å. This distance, in turn, corresponds to the preferential light-induced charge separation pathway between P_{700}^+ and A_{1B}^- in the *B*-branch of the PS I redox cofactors. We suppose that the redirection of electron transfer preferentially from the *A* to the *B* branch of redox cofactors observed in F_X -core complexes embedded in dry trehalose matrix can be rationalized by (1) the lack of the PsaC subunit harboring terminal F_A/F_B 4Fe–4S clusters, which affect the redox properties of A_{1A} and A_{1B} , and (2) selective impairment of the $P_{700} \rightarrow A_{1A}$ electron transfer upon desiccation in trehalose matrix, which is more pronounced in F_X -core complexes.

The results obtained in this work show that desiccation of F_X -core PS I complexes in trehalose matrix does not change the molecular architecture of redox-cofactors, but most probably affects the protein domain around phyloquinone molecules in the A_{1A} and A_{1B} sites and thereby the thermodynamics of electron transfer between P_{700} and A_1 in symmetrical branches of cofactors. Moreover, the results serve as additional argument in favor of the molecular model, which is based on the Le Chatelier–Braun principle, as was proposed in our previous work [1] to rationalize

the cryoprotective effect of trehalose matrix on the functioning of PS I by way of rigidity changes of the hydrogen-bonding network of the protein with the matrix. According to this fundamental thermodynamic principle, local changes in both rigidity and flexibility within complex systems are compensated to establish new thermodynamic equilibria with restored global balance of rigidity and flexibility that is typical for functioning of photosynthetic protein complexes.


Acknowledgements This work was supported by the Russian Foundation for Basic Research (RFBR). K. M. Salikhov acknowledges RFBR Grant 18-43-160017, A. Yu. Semenov RFBR Grant 17-00-00201. K. Möbius acknowledges sustaining support by the Free University of Berlin, Germany. We want to thank Giovanni Venturoli (University of Bologna, Italy) for stimulating and fruitful discussions.

References

1. A.A. Sukhanov, M.D. Mamedov, K. Möbius, A.Y. Semenov, K.M. Salikhov, *Appl. Magn. Reson.* **49**, 1011 (2018)
2. P. Jordan, P. Fromme, H.T. Witt, O. Klukas, W. Saenger, N. Krauß, *Nature* **411**, 909 (2001)
3. G. Palazzo, A. Mallardi, A. Hochkoeppler, L. Cordone, G. Venturoli, *Biophys. J.* **82**, 558 (2002)
4. F. Francia, M. Malferrari, S. Sacquin-Mora, G. Venturoli, *J. Phys. Chem. B* **113**, 10389 (2009)
5. M. Malferrari, A. Savitsky, M.D. Mamedov, G.E. Milanovsky, W. Lubitz, K. Möbius, A.Y. Semenov, G. Venturoli, *Biochim. Biophys. Acta Bioenerg.* **1857**, 1440 (2016)
6. M. Malferrari, A. Nalepa, G. Venturoli, F. Francia, W. Lubitz, K. Möbius, A. Savitsky, *Phys. Chem. Chem. Phys.* **16**, 9831 (2014)
7. A. Savitsky, O. Gupta, M. Mamedov, J.H. Golbeck, A. Tikhonov, K. Möbius, A. Semenov, *Appl. Magn. Reson.* **37**, 85 (2010)
8. G. Cottone, S. Giuffrida, S. Bettati, S. Bruno, B. Campanini, M. Marchetti, S. Abbruzzetti, C. Viappiani, A. Cupane, A. Mozzarelli, L. Ronda, *Catalysts* **9**, 1024 (2019)
9. V. Kurashov, M. Gorka, G.E. Milanovsky, T.W. Johnson, D.A. Cherepanov, A.Y. Semenov, J.H. Golbeck, *Biochim. Biophys. Acta Bioenerg.* **1859**, 1288 (2018)
10. G. Milanovsky, O. Gupta, A. Petrova, M. Mamedov, M. Gorka, D. Cherepanov, J.H. Golbeck, A. Semenov, *Biochim. Biophys. Acta Bioenerg.* **1860**, 601 (2019)
11. G.M. Zhidomirov, K.M. Salikhov, *Sov. Phys. JETP* **29**, 1037 (1969)
12. K.M. Salikhov, S.A. Dzuba, A.M. Raitsimring, *J. Magn. Reson.* **42**, 255 (1981)
13. T. Li, M.B. Tracka, S. Uddin, J. Casas-Finet, D.J. Jacobs, D.R. Livesay, *PLoS ONE* **2014**, 9 (2014)
14. G. Shen, J. Zhao, S.K. Reimer, M.L. Antonkine, Q. Cai, S.M. Weiland, J.H. Golbeck, D.A. Bryant, *J. Biol. Chem.* **277**, 20343 (2002)
15. K.M. Salikhov, I.T. Khairuzhdinov, R.B. Zaripov, *Appl. Magn. Reson.* **45**, 573 (2014)
16. S. Mula, A. Savitsky, K. Möbius, W. Lubitz, J.H. Golbeck, M.D. Mamedov, A.Y. Semenov, A. Van Der Est, *Photochem. Photobiol. Sci.* **11**, 946 (2012)
17. M. Plato, N. Krauß, P. Fromme, W. Lubitz, *Chem. Phys.* **294**, 483 (2003)
18. W. Lubitz, in *Photosystem I*, ed. by J.H. Golbeck (Springer, Netherlands, 2006), pp. 245–269
19. V.V. Ptushenko, D.A. Cherepanov, L.I. Krishtal'ik, A.Y. Semenov, *Photosynth. Res.* **97**, 55 (2008)

Publisher's Note Springer Nature remains neutral with regard to jurisdictional claims in published maps and institutional affiliations.

Affiliations

Andrey A. Sukhanov¹ · **Mahir D. Mamedov**² · **Klaus Möbius**³ ·
Alexey Yu. Semenov^{2,4}  · **Kev M. Salikhov**¹

✉ Alexey Yu. Semenov
semenov@belozersky.msu.ru

✉ Kev M. Salikhov
kevsalikhov@mail.ru

¹ FRC Kazan Scientific Center of RAS, Zavoisky Physical-Technical Institute, Kazan, Russia

² A.N. Belozersky Institute of Physical–Chemical Biology, Lomonosov Moscow State University, Moscow, Russia

³ Department of Physics, Free University Berlin, Berlin, Germany

⁴ N.N. Semenov Federal Research Center for Chemical Physics, Russian Academy of Sciences, Moscow, Russia